J Therm Anal Calorim (2010) 101:779–784
DOI 10.1007/s10973-010-0755-3

Synthesis, thermoanalytical, and spectroscopical studies of dispersed barium titanate

S. Khalameida · V. Sydorchuk · J. Skubiszewska-Zięba · R. Leboda · V. Zazhigalov

IVMTT2009 Special Chapter

Abstract In this article, mechanochemical synthesis of barium titanate from different raw materials was studied. The prepared nanodispersed powders were investigated by means of XRD, DTA-TG, DSC, FTIR, Raman, UV–VIS, ESR spectroscopy, and low-temperature adsorption of nitrogen. Barium titanate possessing high specific surface area was produced directly during dry milling from the mixtures of barium oxides and titanium dioxide low-temperature forms (amorphous and anatase).

Keywords Cubic and tetragonal barium titanate · Mechanochemical synthesis · Phase transitions · –OH defects

Introduction

Barium titanate, $BaTiO_3$ (BT), is one of the most prevalent and popular electroceramic materials. It is used in the preparation of multilayer capacitors, thermistors, sensitive elements of gas and water vapour sensors, catalyst supports, and photocatalysts [1–5]. Its preparation at low temperature in the nanocrystalline powder form, possessing higher specific surface area *S*, is of great interest. Mechanochemical treatment (MChT) is one of the most promising methods used for this purpose. However, only a few works are devoted to address mechanochemical synthesis (MChS) of BT [6–8] and therefore this process has been insufficiently studied. Besides, the presence of defects in the BT structure is also important for its application. These structure defects increase catalytic (including photocatalytic) and adsorption activities of BT. On the contrary, availability of the surface –OH groups or oxygen vacancy strongly impairs ferroelectric properties of BT.

The aim of this study is to synthesize BT in the nanodispersed state and investigate some of its structure characteristics.

S. Khalameida (✉) · V. Sydorchuk · V. Zazhigalov
Institute for Sorption and Problems of Endoecology, NAS of Ukraine, 13 Naumova Str., 03164 Kyiv, Ukraine
e-mail: svkhal@ukr.net

J. Skubiszewska-Zięba · R. Leboda
Faculty of Chemistry, Maria Curie-Skłodowska University, pl. Marii Curie-Skłodowskiej 3, 20-031 Lublin, Poland

Experimental procedure

Mechanochemical synthesis of barium titanate was carried out in the planetary ball mill Pulverisette 6 (Fritsch Gmbh) in air atmosphere for 2–10 h. The amount of milled reagent or mixture of reagents was equal to 10 g. Ten silicon nitride balls with a diameter of 15 mm (total mass was 130 g) and the silicon nitride vessel (250 mL) were used.

Two pathways of mechanochemical BT preparation were used: MChT of barium titanyl oxalate (BTO) produced by "Ferro" company and milling of the mixture of barium and titanium oxides. In the latter case, different compounds of titanium oxide with the specific surface area $S = 4$–$360\ m^2\ g^{-1}$ were used: anatase, rutile, brookite, and their mixtures, metatitanic acid, and amorphous oxide. For comparison, BT powders were also synthesized via hydrothermal (HTT) and microwave (MWT) treatments. HTT was carried out in 45-mL steel autoclaves at 250 °C and under autogeneous pressure for 5 h. For MWT, a high-pressure reactor "NANO 2000" (Plazmatronika, Poland) with power of 650 W was used. The experimental conditions used in this case are as follows: the treatment temperature, 250 °C; pressure, 4.5 MPa; and time, 0.5 h. Then,

all kinds of treatment products were calcined in air at 300–800 °C for 2 h.

The phase composition (XRD) of the obtained samples was determined with a PW 1830 diffractometer (Philips) using CuK_{α} radiation. Thermogravimetric analysis was performed using Derivatograph-C (MOM, Budapest) in air with the heating rate of 10 °C/min in the temperature range of 20–800 °C (sample weight, 50 mg). The FTIR spectra in the range of 4000–450 cm^{-1} were registered using Perkin-Elmer spectrometer "Spectrum One" (pellets with KBr with the mass ratio sample/KBr = 1:20). The specific surface area *S* was calculated using the BET method from the adsorption–desorption isotherms of nitrogen ("NOVA-1200", Quantochrome Instruments). DSC measurements were performed using the thermal analysis system (Differential Scanning Calorimeter, Perkin-Elmer Instruments PYRIS Diamond) at the heating and cooling rate of 50 °C/min from 0 up to 200 °C. The Raman spectra were recorded using RENISHAW Raman Microscope equipped with microscope optical functions. The excited laser line is 514 nm of Ar laser. The electron spectra of the samples were obtained using a UV–VIS SPECORD M 40 spectrometer (Standard, MgO). Electron spin resonance (ESR) was performed using a Bruker ESP 300 spectrometer operating at X-band frequency and 100 kHz field modulation.

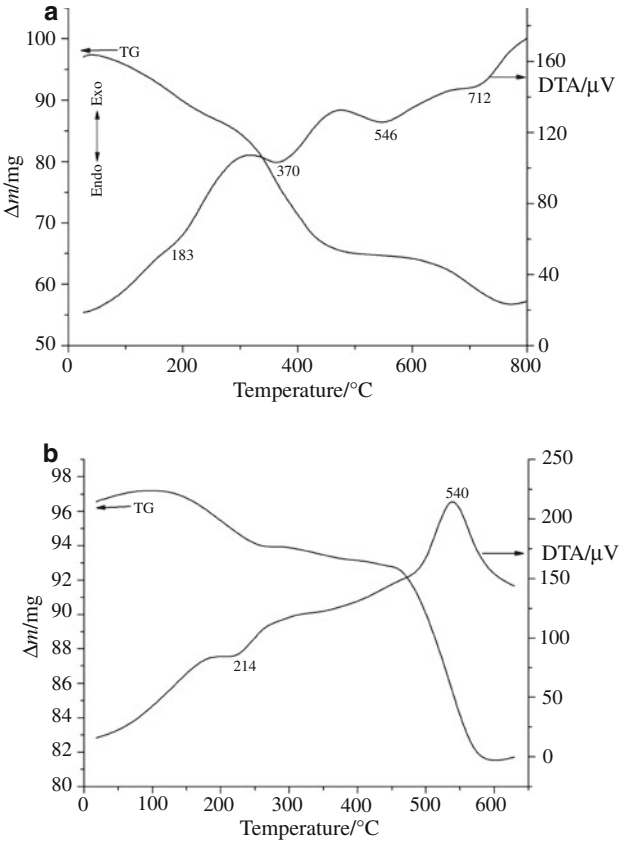

Fig. 1 DTA-TG curves of BTO initial (**a**) and BTO after MChT (**b**)

Results and discussion

In accordance with XRD data, it was established that after 2 h of MChT of BTO, the complete destruction of initial compound crystalline structure takes place. Simultaneously, the appearance of some reflexes of cubic $BaTiO_3$ was observed (diffractograms not shown). The increase of treatment time up to 5–10 h insignificantly changes the intensity of all reflexes on the diffractograms. The complete absence of the reflex corresponding to (101) plane of cubic BT ($d = 0.284$ nm) and some other reflexes of this compound can be due to a defective structure of formed BT. Post-annealing of this BT at 550 °C results in improvement of its structure and appearance of all reflexes characteristic of $BaTiO_3$ with the intensities corresponding to those reported in literature [9]. The XRD patterns of this sample demonstrate no difference with the same BT prepared by conventional thermodestruction of BTO at 800 °C.

The results of thermogravimetric analysis of BTO samples are shown in Fig. 1a and b. The endothermal effects concerned only with BTO thermodestruction are on the DTA-TG curves of the initial sample. At the same time, one can see that the course of DTA-TG curves for milled BTO essentially differs from that for the initial sample. Thus, the exothermal effect at 540 °C on the DTA curve of milled samples can be related to crystallization of the amorphous part of BT formed during MChT.

The FTIR spectra shown in Fig. 2 also confirm the formation of BT after milling of BTO. As can be seen, the spectrum of the product obtained by MChT for 5 h (Fig. 2, curve *b*) differs drastically from that of the starting spectrum of BTO (Fig. 2, curve *a*): all absorption bands of BTO (wide bands 560, 859, and 1056 cm^{-1}) are absent in the spectrum of the obtained product. At the same time, in the spectrum of milled sample, the absorption bands characteristic of BT, i.e., 488, 527, and 908 cm^{-1}, are present [10]. Thus, the results obtained from XRD, DTA-TG, and FTIR spectroscopy can indicate the fact that part of amorphous BT is present in the products of MChT of BTO.

MChT of mixtures of BaO with various modifications of TiO_2 also led to the formation of cubic BT in all cases; however, if the brookite, rutile, or rutile–anatase mixtures were used as the initial TiO_2-containing compounds, the presence of these oxides in the treated samples was also observed (see, for example, Fig. 3, curve *d* and Table 1). The use of anatase, amorphous TiO_2, or anatase–brookite mixture results in the formation of BT only (Fig. 3, curves *a–c*, and Table 1).

BT that is formed during milling and following annealing (up to 800 °C) is cubic. However, study of the

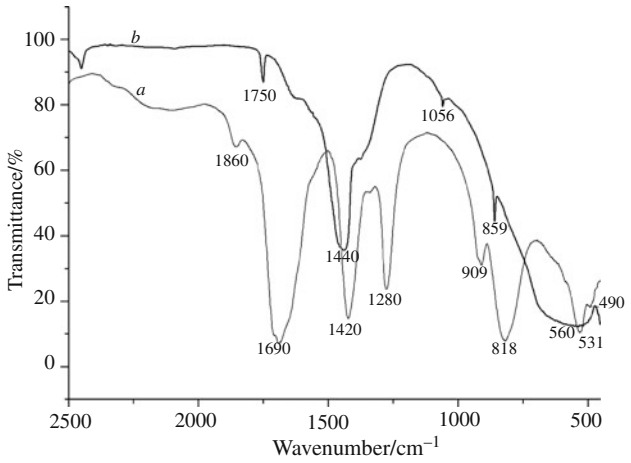

Fig. 2 FTIR spectra of BTO: initial (*a*) and milled in air for 5 h (*b*)

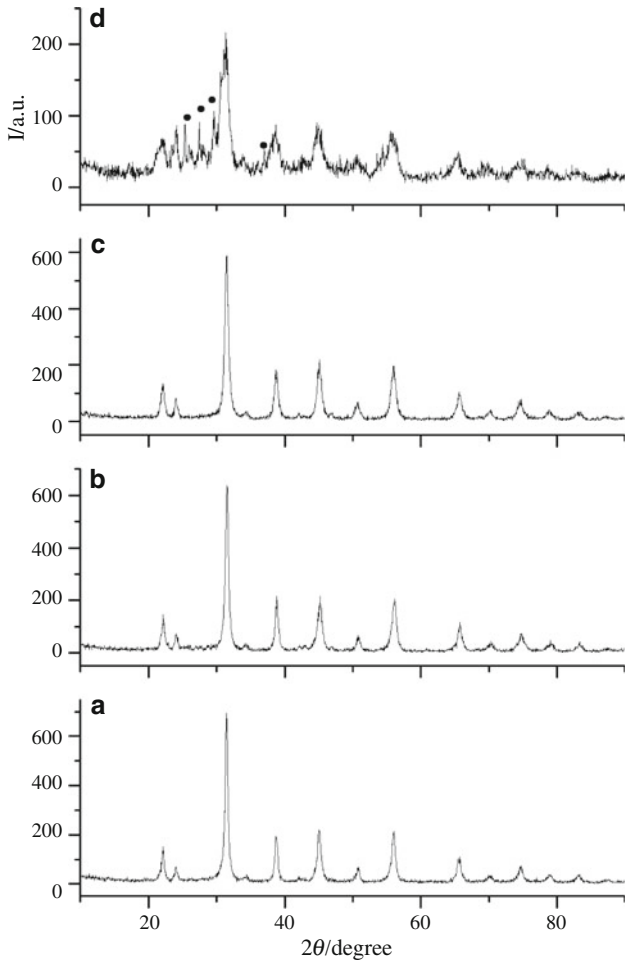

Fig. 3 XRD patterns of BT prepared by **II**: TiO_2 = B + A (**a**), TiO_2 = A (**b**), TiO_2 = amorph. (**c**), and TiO_2 = A + R (**d**). The reflexes of initial oxides marked by *bullets*

samples prepared from the mixtures composed of barium oxide and titanium dioxide (anatase and brookite) by means of Raman spectroscopy indicates following. Spectrum contains absorption bands corresponding stretching modes 303 B_1, E(LO + TO), 517–520 E(TO), A_1(TO) and 717–722 E(LO), A_1(LO) cm^{-1} (Fig. 4) which are assigned to tetragonal BT [11, 12]. Thermal treatment leads to diminution of the amount of cubic phase and increasing of the tetragonal phase content. Appearance of a wide band 245–248 cm^{-1} which correlates with the mode TO of A_1 symmetry is the confirmation of that tendency. The bands ~520 and 717 cm^{-1} appear in the spectra of both cubic and tetragonal modifications. Thus, during MChS, cubic BT with inclusion of tetragonal BT and lattice defects namely, centers of local symmetry of tetragonal phase is formed.

The XRD data indicate that cubic BT appeared as a result of hydrothermal and microwave treatments of BaO mixtures with different kinds of TiO_2, which is in agreement with literature data [13–15]. However, analogous to the milled BT powders, Raman spectra of these samples are composed of absorption bands assigned to both cubic and tetragonal modifications. The XRD diffractograms and Raman spectra of the samples prepared via HTT and MWT are similar to those for milled BT and therefore are not presented here.

It is known [10] that cubic BT is metastable at 25 °C. The presence of defects, for example –OH groups, causes its existence under such conditions. The DTA-TG (Fig. 5) and FTIR (Fig. 6) data confirm this supposition. One can see that on the DTA curve in the range of 400–600 °C endothermal effect accompanied by mass loss equal to 1.8% w/w on the TG curve. This mass loss corresponds to removal of surface and lattice –OH groups, which is in agreement with literature data [12, 16].

The FTIR analysis of BT powders also shows, as a rule, a broad resonance for the –OH stretching vibration in the range of 3000–3600 cm^{-1}. In the spectrum of the sample prepared via milling of the samples produced using the mixture containing TiO_2 in the anatase and brookite forms, a broad band with the maximum at 3490 cm^{-1} appears (Fig. 6, curve *a*). It is assigned to the surface-adsorbed –OH groups because of their adsorption on many surface sites [17]. Annealing of such milled BT at 600–800 °C results in disappearance of this band (Fig. 6, curves *b*, *c*). At the same time, intensity of the band at 1447 cm^{-1} sharply decreases; however, it appears in the spectrum after calcinations up to 800 °C. This band relates to the vibration of CO_3^{2-} groups [18] which are always contained in BT synthesized in air and aqueous solutions as impurity. The absorption band of CO_3^{2-} groups is also present in the Raman spectra (1059 cm^{-1}). Therefore, annealing of BT powders promotes elimination of the defects such as –OH and CO_3^{2-} groups.

Meantime, defects of different nature appear in the temperature range of 400–600 °C due to dehydroxylation

Table 1 Properties of some BT powders prepared by MChT

Sample no.	Treatment	$S_{TiO}/m^2\ g^{-1}$	PhCaT	I_{101}/I_{002}	D_{101}/nm	$S/m^2\ g^{-1}$	D_S/nm
1	BTO thermodestruction (700)	0.1	BTO + BT	100/31	15.7	6.8	147
2	BTO thermodestruction (800)		BT	100/26	16.8	5.3	208
3	BTO MChT 5 h		BT	0/100	–	23.1	43
4	BTO MChT 5 h + annealing (550)		BT	100/29	15.0	19.6	51
5	BTO MChT 5 h + annealing (700)		BT	100/31	16.5	17.5	57
6	BTO MChT 5 h + annealing (800)		BT	100/36	18.5	14.2	70
7	Mixture MChT 5 h, TiO_2 = B + A	54	BT	100/28	18.0	48.0	21
8	Mixture MChT 10 h, TiO_2 = B + A		BT	100/32	13.2	49.0	20
9	Mixture MChT 5 h, TiO_2 = A + R	65	BT + R	100/40	7.8	79.0	13
10	Mixture MChT 5 h, TiO_2 = amorphous	380	BT	100/37	12.0	65.0	15
11	Mixture MChT 5 h, TiO_2 = A	103	BT	100/36	15.1	45.0	22

S_{TiO} specific surface area of initial Ti-containing reagents, *PhCaT* phase composition of the samples after treatment, D_{101} crystallite size calculated from XRD data, S_{BaTiO3} specific surface area of treatment products, D_S effective particle size calculated from S_{BaTiO3}, *B* brookite, *A* anatase, *R* rutile

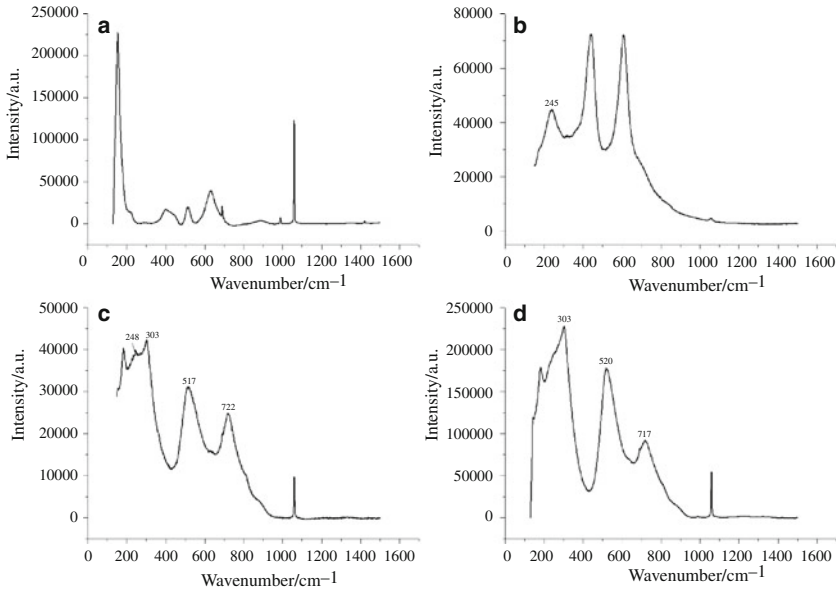

Fig. 4 Raman spectra patterns of BT prepared by solid-state interaction at 1100 °C (**a**), and after MChT for 3 h (**b**), 5 h (**c**), and 10 h (**d**)

processes. Thus, the signal with g-factor equal to 1.96630 is registered in ESR of milled BT samples. Intensity of this signal depends on temperature following the thermal treatment: its value decreases for the samples annealed at 300–400 °C, rises after calcination at 600 °C, and again diminishes for the samples calcined at 800 °C. Appearance of ESR signal is obviously associated with formation of Ti^{3+}–oxygen vacancy pair [19]. Reduction of its intensity can be related with relaxation of these defects.

It should be noted that parameters such as permittivity ε and band gap E_g presented in Table 2 change in coordination with the intensity of ESR signal. It is clear since the value of ε is very sensitive to availability of structure defects in BT [1]. On the other hand, the value of band gap calculated from the absorption edge λ also varies. The latter parameter was determined from the UV–VIS spectra [20]. In accordance with these spectra, shift of absorption edge toward the visible region is observed for the milled and annealed samples at 400–600 °C which leads to narrowing of band gap. At the same time, calcination at 800 °C accompanied by relaxation of defects results in formation of BT powders possessing E_g approximate to that for monocrystalline BT.

Origination of BT tetragonal directly on the milling stage is also verified by DSC [12, 21, 22]. Phase transition of BT tetragonal-cubic occurs at Curie temperature

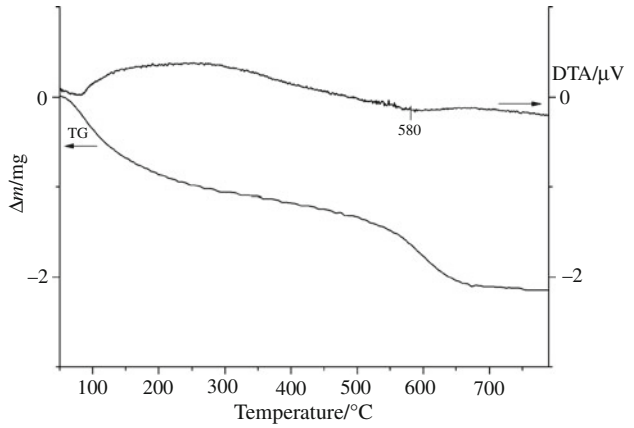

Fig. 5 DTA-TG curves of BT sample prepared via MChS from anatase + brookite

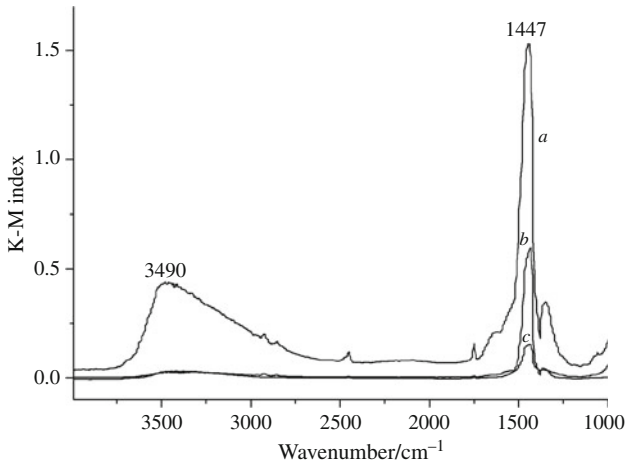

Fig. 6 FTIR spectra of BT prepared via MChT (*a*), and the next thermal treatment at 600 °C (*b*) and 800 °C (*c*)

Table 2 Some properties of the sample prepared by MChS from BaO with TiO_2 (anatase with brookite) and calcined at different temperatures

	Temperature/°C						
	As received	300	400	500	600	700	800
S/m^2 g^{-1}	48	42	38	35	31	26	21
E_g/eV	2.70	2.87	2.79	–	2.75	2.80	2.93
ε	11	18	20	16	12	21	29

(130 °C) for the sample obtained via milling of mixture containing anatase and brookite (Fig. 7). The calculated enthalpy ΔH of this transition equals to 3 mJ g^{-1}. Meanwhile, $\Delta H = 550$ mJ g^{-1} for monophase BT [12]. The comparison of these values also indicates that only the inclusions of tetragonal phase are formed in the stage of milling.

The data presented in Table 1 show that the samples prepared by MChT in both ways have the higher values of

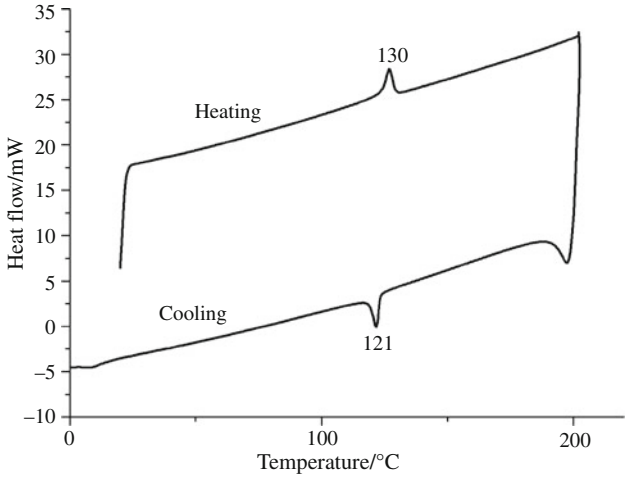

Fig. 7 DSC data of BT prepared via MChT of the mixture containing anatase and brookite

specific surface area and simultaneously smaller size of particles D_s and crystallites D_{hkl} than the sample obtained as a result of conventional calcination (Table 1, sample no. 2). The increase of annealing temperature for the milled samples causes lowering of specific surface area and particle dimensions (Table 1, samples nos. 4–6) but their values remain much larger and smaller, respectively, than for the sample prepared by the traditional solid-state technique. At the same time, powders synthesized from oxide mixtures possess the maximal specific surface area. Some correlation between the values of specific surface area of formed BT and the initial TiO_2 is found. Besides, the comparison of D_{101} and D_s indicates the weak aggregation of crystallites in the case of milling of oxide mixtures.

On the other hand, BT powders produced through HTT and MWT possess relatively not large values of specific surface area, namely, 10–20 m^2 g^{-1} that can be explained by hydrothermal conditions of recrystallization processes.

Conclusions

It is established that chemical interaction of barium and titanium oxides with formation of nanocrystalline barium titanate possessing high specific surface area takes place during dry mechanochemical treatment of oxide mixtures. Milled products represent cubic BT with inclusions of tetragonal modification, which is proved by means of XRD, Raman spectroscopy, and differential scanning calorimetry. The presence of structure defects in the form of –OH and CO_3^{2-} groups and Ti^{3+} ions which was studied by means of DTA-TG, FTIR, UV–VIS, and ESR spectroscopy influences on some important characteristics of prepared powders.

Acknowledgements This work was partly supported by International Visegrad Fund (Contract No 50810086).

References

1. Rae A, Chu M, Ganine V. Barium titanate: past, present and future. Ceram Trans. 2007;100:1–12.
2. Moreno J, Dominguez JM, Montoya A. Synthesis and characterization of $MTiO_3$ (M = Mg, Ca, Sr, Ba) sol-gel. J Mater Chem. 1995;5:509–12.
3. Yohichi Y, Masaru T, Masato K. Synthesis RuO_2-loaded $BaTi_nO_{2n+1}$ (n = 1, 2, 5) using a polymerizable complex method and its photocatalytic activity for the decomposition of water. J Mater Chem. 2000;12:1782–6.
4. Yuk J, Troczynski T. Sol-gel $BaTiO_3$ thin film for humidity sensors. Sens Actuators B. 2003;94:290–3.
5. Luxová J, Šulcová P, Trojan M. Study of perovskite compounds. J Therm Anal Calorim. 2008;93:823–7.
6. Welham NJ. Mechanically induced reaction between alkaline earth metal oxides and TiO_2. J Mater Res. 1998;13:1607–13.
7. Xue J, Wang J, Wan D. Nanosized barium titanate powder by mechanical activation. J Am Ceram Soc. 2000;83:232–4.
8. Stojanovic BD, Simoes AZ, Paiva-Santos CO, Jovalekic C, Mitic VV, Varela JA. Mechanochemical synthesis of barium titanate. J Eur Ceram Soc. 2005;25:1985–9.
9. Khollam YS, Deshpaude AS, Potdar HS. A self-sustaining acid-base reaction in semi-aqueous media for synthesis of barium titanyl-oxalate leading to $BaTiO_3$ powders. Mater Lett. 2002;55:175–81.
10. Mullens J, Van Werde K, Vanhosland G. The use of TGA-MS, TGA-FTIRHT-XRD and HT-DRIFT for the preparation and characterization of $PbTiO_3$ and $BaTiO_3$. Thermochim Acta. 2002;392–393:29–35.
11. Lagos P, Hermans R, Velasco N, Tarrach G, Schlaphof F, Loppacher C, et al. Identification of ferroelectric domain structures in $BaTiO_3$ for Raman spectroscopy. Surf Sci. 2003;532–535:493–500.
12. Frey MH, Payne DA. Grain-size effect on structure and phase transformations for barium titanate. Phys Rev B. 1996;54:3158–68.
13. Boulos M, Guillemet-Fritsch S, Mathieu F, Durand B, Lebey T, Bley V. Hydrothermal synthesis of nanosized $BaTiO_3$ powders and dielectric properties of corresponding ceramics. Solid State Ionics. 2005;176:1301–9.
14. Jhung S, Lee J, Yoon J, Hwang Y, Hwang J, Park S, et al. Effects of reactions in microwave synthesis of nanocrystalline barium titanate. Mater Lett. 2004;58:3161–5.
15. Aoyagi S, Kuroiwa Y, Sawada A, Kawaji H, Atake T. Size effect on crystal structure and chemical bonding nature in $BaTiO_3$ nanopowder. J Therm Anal Calorim. 2005;81:627–30.
16. Badheka P, Qi L, Lee B. Phase transition in barium titanate nanocrystals by chemical treatment. J Eur Ceram Soc. 2006;26:1393–400.
17. Noma T, Wada S, Yano M, Suzuki T. Analysis of lattice vibration in fine particles of barium titanate single crystals including lattice hydroxyl group. J Appl Phys. 1996;80:5223–9.
18. Balaz P, Plesingerova B. Thermal properties of mechanochemically pretreated precursors of $BaTiO_3$ synthesis. J Therm Anal Calorim. 2000;59:1017–21.
19. Gesenhues U. The effects of plastic deformation on band gap, electronic defect states and lattice vibrations of rutile. J Phys Chem Solids. 2007;68:224–35.
20. Liu G, Li F, Chen Z, Lu GQ, Cheng H-M. The role of NH_3 atmosphere in preparing nitrogen-doped TiO_2 by mechanochemical reaction. J Solid State Chem. 2006;179:331–5.
21. Baeten F, Derks B, Coppens W, van Kleef E. Barium titanate characterization by differential scanning calorimetry. J Eur Ceram Soc. 2006;26:589–92.
22. Radecka M, Rekas M. Microcalorimetry studies of phase transitions in $(Ba_xSr_{1-x})TiO_3$. J Therm Anal Calorim. 2007;88:731–4.